24th ABCM International Congress of Mechanical Engineering
December 3-8, 2017, Curitiba, PR, Brazil

COBEM-2017-1881
CONTROL OF A TENDON-DRIVEN ROBOTIC HAND FROM SURFACE ELECTROMYOGRAPHIC SIGNALS

Carlos Gerardo Paucar Malqui[1]
Marco Antonio Meggiolaro[2]
Pontifícia Universidade Católica do Rio de Janeiro, Department of Mechanical Engineering, Rio de Janeiro, Brazil
[1]carlos.paucar@hotmail.com, [2]meggi@puc-rio.br

Abstract. *Initially, this research was presented as main study to develop a robotic prosthesis for people with hand amputation, such as the case of disjointed amputation handle. This paper covers the following topics: position of electrodes to capture the surface electromyography signals (sEMG), design of an electromyography as muscle interface, pre-processing method and the use of techniques of computational intelligence for the interpretation of the sEMG signals, design of the robotic hand and control method used to control the positions of the fingers and the control of hand grip strength. Was used the wavelet packet as feature extraction method in electromyographic signals, and multi-layer neural network as pattern classification method. The proposed model obtained satisfactory results, thereby capturing 90.5% for recognizing positions of 6 different hand positions 5 to 94.3% and 96.25% for 4 positions.*

Keywords: *Surface electromyography, Patterns Classification, Neural Networks, Wavelet Transform, Robotic Hand.*

1. INTRODUCTION

In the last years, robotics had great importance in the area of medicine, developing artificial equipment and devices that are increasingly similar to the functions of natural organs, is developing robotic members in different projects: mechanical arms with movements increasingly similar to those of natural arms; Advanced robotic hands capable of reproducing the functional capabilities of the human hand; Artificial legs controlled with commands, even surrogate hands and feet, more and more advanced.

But, besides the numerous and wonderful technological advances in the field of rehabilitation engineering, prosthetic robotic hand today becomes a little large in relation to the human hand, acting as a load at the end of the arm. The structural complexity of the skilled robotic hands leads to high costs and very basic reliability in the developed prototypes (Douglas G. Smith, 2006).

Table 1. Main features of robotic hand.

Hand name	Mass (g)	Nominal size	Number actuators	Number fingers	Number sensors	Number DOF
Human(1)	≈ 400	1	38	5	17000	22
RTR1	250	»1	6	3	9	8
RTR2	350	>1	2	3	2	10
Spring	400	»1	1	3	1	8
Cyberhand	450	≈1	6	5	44	16
DLR2	320	≈1.5	13	4	64	13

(1) data of the human hand as the main reference (G.L. Taylor, R.J.Schwart, 1955)

In the quest to reduce the size and mass of hand prostheses in the current market, and according to the technological limitations of our time, the present work proposes to design a robotic system that fulfills the basic functions of the human hand, by training a set of common and repetitive patterns of the human hand. This is driven by tendons that are driven by direct current (DC) motors, which are the actuators, which in turn are controlled by surface electromyographic signals. Robotic hand incorporates force control to do basic gripping tasks.

It proposes a mechanical structure based on a sub-actuated mechanism, which requires fewer actuators without reducing the number of degrees of freedom. This allows the fingers of the robotic hand is able to adapt to the morphology of the object, thus achieving a greater hand flexibility, a simpler control, and reduced mass.

To achieve this goal, the following steps must be performed: implementation of an electromyography system; development of an interface for the pre-processing and processing of electromyographic signals; construction of a robotic hand with sensory system; integration of the electromyography system with the robotic hand.

2. IMPLEMENTATION OF ELECTROMYOGRAPHY SYSTEM

Electromyography is the technique used to measure and record muscle response, it measures electrical activity within muscle fibers, muscle stimulation caused by nerve impulses at rest and during contraction (Peter Konrad, 2005).

In this work, the superficial (non-invasive) electromyography technique was used to measure the electrical activities of a patient's muscles, using passive Ag/AgCl disc electrodes with 10 mm diameter. To avoid interferences with cross-talk signals, said electrodes were used with a separation of 20 mm, according to the recommendations of the SENIAM standard (R.Merletti, P. Parker, 2004). The muscles were: extensor carpi radialis, palmaris longus, extensor digitorum conmunis, as shown in Fig. 1.

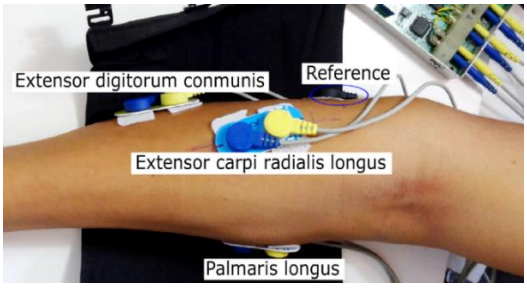

Figure 1. Location of the Ag/AgCl electrodes in the forearm

For the implementation of the electromyography system, an acquisition system was developed with the following characteristics: three channels of differential mode input, with protection circuit in the input to electrically isolate the patient from the power line or the battery, so that it is Protected from an electric shock produced by the equipment in the event of an error; a stage of conditioning the sEMG signals to amplify their reduced magnitude and to filter out the different noises affecting them; and a final stage with the signal of the digitization process, with 2 kHz, sampling frequency, developed in NI9012 CompactRIO system with the help of NI9205 acquisition module that features 16-bit resolution.

The filtering stage is composed of a 2-order *Butterworth* low-pass filter at 577 Hz cut-off frequency to eliminate high-frequency components and avoid aliasing, and composed of a *Butterworth* high pass filter of order 2 at a cut-off frequency of 15.6 Hz to eliminate noise coming from neighboring muscles, and potential repolarization of muscles, these filters are connected in cascades.

Table 2. Features of the electromyography system.

Low pass filter	fc = 577 Hz
High pass filter	fc = 15.6 Hz
Gain	31.5 - 3180
CMRR	130 dB (min)
Conversion resolution A/D	16 Bits

In the conditioning stage, a signal pre-amplifier was used as the myoelectric signals are in the range of 200 µV-10 mV peak-to-peak and noises or apparatus such as ambient noise can cause a false interpretation of the results. At this stage using an instrumentation amplifier INA114 *Texas Instruments* so that it has a high CMRR of about 100 dB with a gain value of 31, and is more than enough for our design (Texas Instrument, 2000).

We use the RLD circuit, with the purpose of placing the patient in the same potential of the electric circuit, to avoid problems of electric discharge, to minimize noise generated by the common mode potentials that appear when the patient's body is not grounded or is not in the Reference potential of the amplifiers (Talles M. G., 2008).

We also used an amplification circuit to increase the magnitude of the sEMG signals collected. The scheme of this stage is a negative feedback non-inverting amplifier that produces a larger input impedance increase and a decrease in output impedance (Albert Malvino, 1998). In the scheme, a potentiometer was used to have the possibility to control the gain.

The Pspice A/D software was used to simulate and verify the correct functioning of the protection circuit.

For the design of the printed circuit board (PCB) was used *Eagle* implemented SMD component to obtain a reduced size (see Fig. 2).

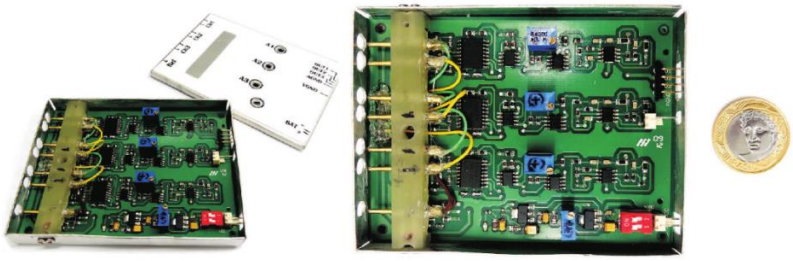

Figure 2. Final printed circuit of the Electromyography system.

3. PRE-PROCESSING OF THE SEMG SIGNAL

Muscle activity data were collected in 400 ms times, by the electromyography system, enough time to collect samples that determine a type of hand position pattern. To reject high-frequency noise an eighth-order Butterworth digital low-pass filter was implemented with final passband frequency (f_P) at 400 Hz, initial rejection band frequency (f_S) at 600 Hz, bandpass deviation (δ_P) at -1 dB, and rejection band deviation (δ_S) at -20 dB. To reject the electric line noise, the digital notch filter was used with sampling rate at 2 kHz, rejection frequency at 60 Hz and quality factor of 12. We use an evaluation method to identify whether the collected signal represents a pattern, to be directed to a processing stage or simply to be discarded.

The block diagram shown in Fig. 3, shows the process sequence in the pre-processing stage.

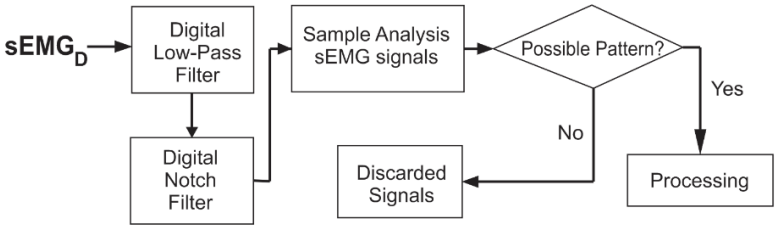

Figure 3. Block diagram of the preprocessing phase.

In the evaluation method, we used the root mean square value (RMS), a statistical measure used to analyze the magnitudes of the sub-samples, extracted from a sample of the sEMG signal. In Figure 4, we show 4 sub-samples that are analyzed to determine whether or not they undergo much variation over the length of the signal. In the case of the figure, it can be seen that it is a signal in transition from one posture to another and the sample would have to be discarded.

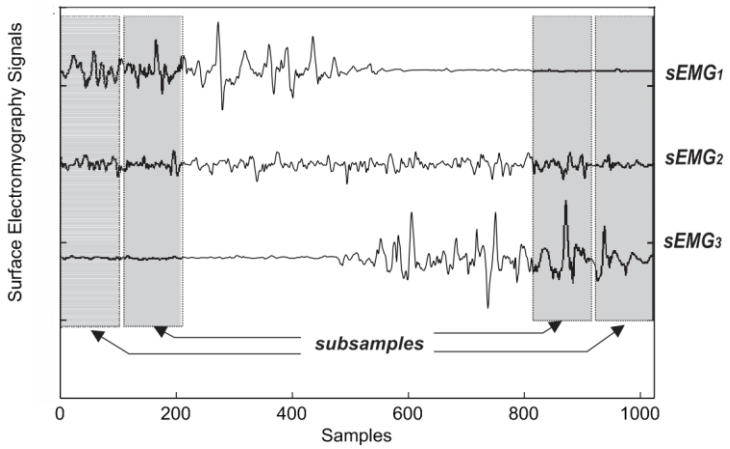

Figure 4. Sampling analysis of the digitized sEMG signal.

Being x[n] sign on $n_1 \leq n \leq n_2$ time interval, the RMS is defined as:

$$RMS = \sqrt{\frac{1}{n_2 - n_1}\sum_{n=n_1}^{n_2} x[n]^2} \quad (1)$$

We calculated the mean RMS value of the M sub-samples from the sample collected for an sEMG signal.

$$\overline{RMS} = \frac{1}{M}\sum_{i=1}^{M} RMS_i, \qquad i = 1,2,\dots,M \quad (2)$$

To validate the signal, we use the relative value of the (rms_i) sub-sample, we use the following Eq. (3):

$$rms_i = \frac{RMS_i}{\overline{RMS}} \quad \text{and} \quad |rms_i - 1| < \theta_{error} \quad (3)$$

Where θ_{error} is the admissible error value as the maximum limit.

From the RMS we will use the $\overline{P}$ (Alan V. Oppenheim, 1997) mean power concept to estimate the total energy value of the samples.

$$\overline{P} = \frac{1}{M}\sum_{i=1}^{M} RMS^2, \qquad i = 1,2,\dots,M \quad (4)$$

The calculation of the ($\overline{E_T}$) total energy of the three electromyographic signals for our analysis is calculated with:

$$\overline{E_T} = \left(\overline{P_{sEMG1}} + \overline{P_{sEMG2}} + \overline{P_{sEMG3}}\right)xN \quad (5)$$

Where N is the total number of data in a sample.

For our analysis of the sample of the sEMG signal we use the following logical rules (6). We determine as a possible pattern when it complies with the (3) and (6) equations, and if it is not determined by default, the robotic hand remains in the same position.

$$Output: \begin{cases} if\ \overline{E_T} > \theta_{Emax} & ; Possible\ pattern. \\ if\ \overline{E_T} < \theta_{Emin} & ; Pattern: relaxed\ hand. \\ Another & ; is\ not\ pattern. \end{cases} \quad (6)$$

Where θ_{Emax} and θ_{Emin} are respectively the maximum value and the minimum allowable energy value, and are calculated experimentally as is θ_{error}.

To estimate the parameters of the Eq. (3) and (6), a sEMG signal database shown in Tab. 3 was used. With the help of the total energy bloxplot plot (see Fig. 6), estimated from the records for each pattern, the parameters θ_{error} = 0.6 (60%), θ_{Emax} = 10 and θ_{Emin} = 2 were determined, knowing that the data size for each sample was N=1024, and from each sample 4 sub-samples were extracted (M=4).

Table 3. Results for 60% of permissible error and 100 ms of analyzed for each sub-sample.

Name of Pattern	Number of Samples	Well defined (%)	Average value Total Energy	Maximum value Total Energy
Extension	223	91.03	26.15	109.85
Flexion	226	96.02	26.88	88.06
Like hand	231	83.98	12.45	77.07
Make fist	223	90.13	42.40	192.05
Spherical	225	98.67	51.40	161.48
Spread	208	94.23	16.09	44.58

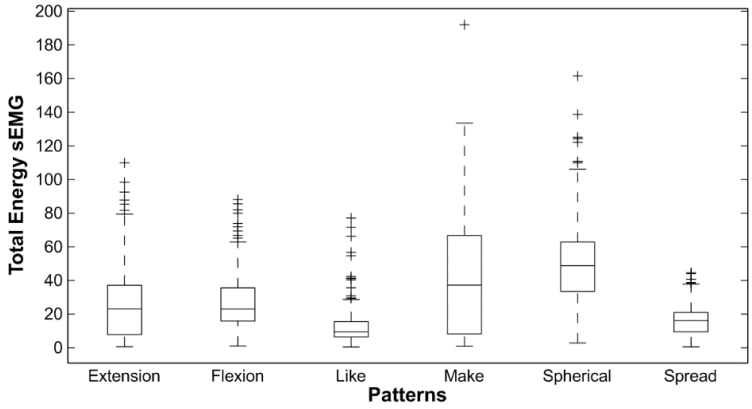

Figure 5. Boxplot of the estimated total energy of the database.

4. PROCESSING OF THE SEMG SIGNAL

In the processing stage, the wavelet transform method is used as the extraction of characteristics of the preprocessed sEMG data and the neural networks as a classification method (see Fig. 6).

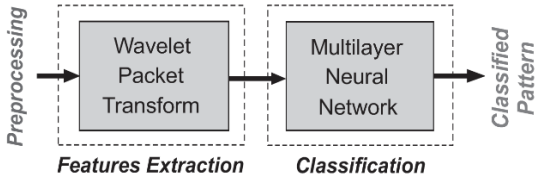

Figure 6. Block diagram of the processing phase.

4.1 Feature Extraction

In the method of extraction of characteristics, we use the wavelet transform with the help of the wavelet daubechies base function of order 6, thus creating a decomposition tree, as shown in Fig. 7.

For our signal that presents a sampling frequency F_S=2 kHz with N=1024 data in the sample, we use the wavelet transform with decomposition tree up to level 7, with reference to the fact that the maximum decomposition level is 10 ($\log_2$N=10). In level 7, the frequency range of each node has a difference of Δf = 15.625 Hz between the nodes, where we chose to select those nodes with frequency bands of interest for our processing.

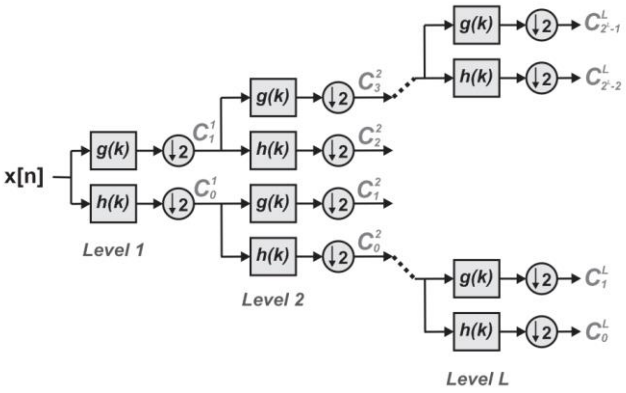

Figure 7. Analysis of the filter bank tree that leads to wavelet packets.

$C_n^l(k)$ are the coefficients of the wavelet transform for a node, determined for a decomposition level *l*, *n* as node location index within a decomposition level, and *k* as the vector index of the coefficient of the wavelets transform (see Fig. 8).

According to the general concepts, the harmonics of interest of the sEMG signal are approximately in the frequency range 16 Hz-400 Hz, therefore, from the wavelet packets tree it is determined the use of the nodes in the level 7, which

allows us to select a set of nodes with frequencies contained in the desired range. As a result, we get the frequency range 15.625 Hz-406.25 Hz. At level 7, the first node ($C_0^7: 0 - 15.625\ Hz$) and nodes with frequencies greater than 406.25 Hz (C_{26}^7 for above) were disregarded.

In the Equation (7), we calculate the energy of the (E_W^i), wavelet coefficients, using all the nodes selected at the depth level of the wavelets tree studied for an electromyographic signal register.

$$E_W^i = \sum_{n=1}^{25} \sum_{n=1}^{25} |C_n^7(k)|^2, \qquad i = 1, 2, 3 \tag{7}$$

Where *i* indicates the channel number used to acquire the sEMG signal records (remember that 3 channels were used). We obtain E_W^1, E_W^2 and E_W^3 respectively from the electromyographic records $sEMG_1$, $sEMG_2$, $sEMG_3$ and calculate the total energy of the wavelet coefficients E_W^T for the three signals studied, according to the Eq. (8).

$$E_W^T = E_W^1 + E_W^2 + E_W^3 \tag{8}$$

With Eq. (7) and Eq. (8) we calculate the relative energy of the wavelet coefficients ($\overline{E}_W^i = E_W^i / E_W^T$) and obtain $\overline{E}_W^1$, $\overline{E}_W^2$ and $\overline{E}_W^3$ to be used as characteristic value in the training and decision on the classification system.

Our pattern classification system is based on the multi-layer artificial perceptron neural network (MLP) model. From a database created, our classification system was modeled to determine six different positions (Fig. 8) in which we also call patterns.

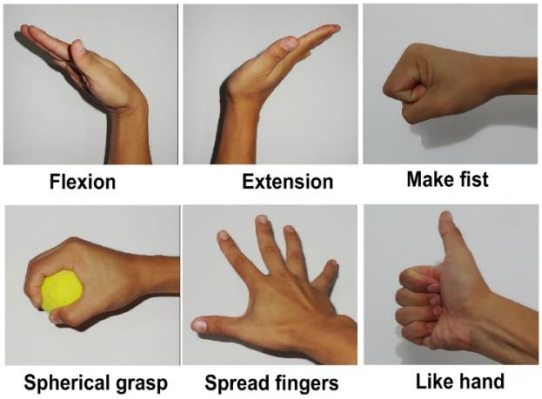

Figure 8. Types of hand positions to be used as recognition patterns.

We use the WEKA software to search for the best configuration of our classification model and to validate it in comparison with other different methods; K-nn (K nearest neighbours) method,Naive Bayes classification method, C4.5 (known as J48) algorithm. From the database, different data sets were created to train the classification models in the recognition of 6 patterns, 5 patterns and 4 patterns, with a learning rate of 0.3, momentum in 0.2 and different training times for all the configurations of our neural network model. We obtain the following Tab. 4, where we can observe the best models of the three groups. The parameter values of the K-nn, C4.5 and Naive Bayes models are predefined values of the WEKA software.

Table 4. Recognition percentage in 3 groups of patterns with different sorting methods.

Number of Pattern	%K-nn	%C4.5	%Naive Bayes	%MLP
6 Patterns	81.11	84.07	80.37	87.78
5 Patterns	87.72	89.04	86.40	92.55
4 Patterns	88.52	93.44	90.16	94.00

5. DESIGNING AND BUILDING OF THE ROBOTIC HAND

The architecture of the robotic hand operating system was designed according to Fig. 9. It is composed of the following parts: the processing system responsible for carrying out all the operations necessary for the operation of the robotic hand, which stores and executes the control algorithms; the input and output modules that are used as interface between the devices and elements external to the processing system; sensors and actuators; and a power source for the system.

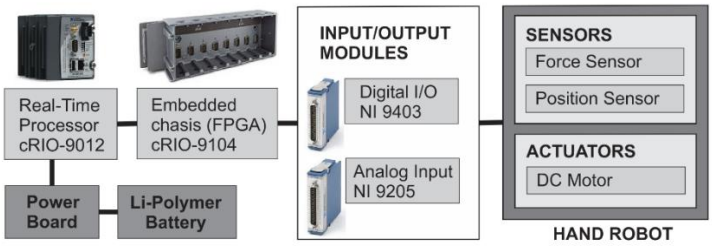

Figure 9. Architecture of the robotic hand operating system.

The mechanical structure of the robotic hand, is composed of five fingers (index, middle, ring, minimum and thumb), and was taken into account the following concepts for its projection: it should be self-contained, the robot hand must be an independent piece, as yet should not have external tendons or transmission elements to the same hand; it should be anthropomorphic, the robotic hand should have the appearance of the human hand; and the dimensions should be as close as possible to the human hand. Due to the complexity of the movements presented by the fingers of the hand, the abduction and adduction movements of the fingers were excluded, excluding the thumb, which complies with the abduction and adduction movements, as well as the flexion and extension movements.

Taking into account all these aspects, the robotic hand is designed in SolidWorks Simulation software is built with tubes and aluminum profile as the main material. We used a steel tape that fulfills the function of flexion of the finger, and to achieve its linear movement we use a system based on pulleys of transmission and worm, where from the rotational movement of the motor we can have linear movement through the worm screw.

The pulleys are anodized aluminum with good corrosion resistance and trapezoidal teeth with a 0.080" spacing between the teeth. The screw used is bronze with a minimum tensile strength of 55000 psi, is 1/4" in diameter and 1 mm pitch.

As actuators we used the Pololu Micro Metal Gearmotor HP motor of the motor-reducer type with parallel rotor that work in 6 V and we used the driver L298 of the ST Microelectronics to drive them.

The position sensors used for the index, middle, annular and minimum fingers are a simple flexibility sensor that changes its resistance between its terminals as it bends it, its resistance increases depending on the amount of curve you experience.

The resistance variations of this sensor are unidirectional and range from 60 kΩ to 110 kΩ, have a tolerance of $\pm$30% and can be used within the temperature range of -35°C to 80°C. To measure the movements of the thumb, we used two potentiometers to determine the angular positions of two gearmotors.

The force sensor used was the resistive type FSR 400 of 0.5" diameter sensitive area. This component varies its resistance (in ohms Ω), as applying force on its surface.

To prepare the measurements of the sensors, basic circuit structures with operational amplifiers were used, based on a simple voltage divider and a voltage follower, in order to increase the voltage difference at the sensors output, to obtain a very high resistance of Input and very low output resistance, thus isolating the circuit.

Biomechanical analysis of the finger was used with the aid of image processing, recognizing the trajectory of red dots that were glued to the points that represent the axes of the finger joints, besides, the signal of the flexibility sensor was collected, located on the finger and then those data were compared with the kinematic data obtained from the biomechanical analysis.

In Figure 10, *y* represents the linear displacement of the worm, and y_0 is the initial position for the finger flexion movement. The steel strip angularly displaces the θ_1, θ_2, and θ_3, (see Fig. 10.a) joints, thus providing a great handling capacity (see Fig. 10.b).

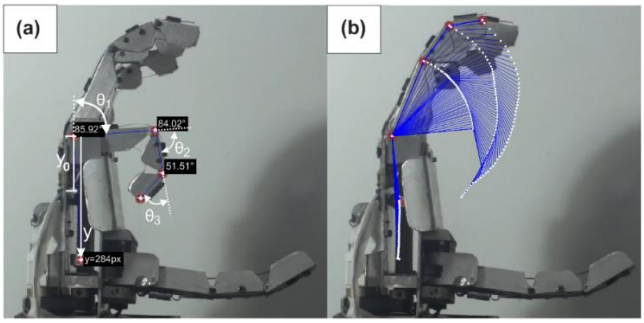

Figure 10. Representation of the index finger. (a) Setting the index finger; (b) Trajectory of the index finger.

In the biomechanical analysis of the finger, made with video recording of 29 frames per second, the relation of the angles at the joints between the (θ_1, θ_2, and θ_3) finger phalanges was obtained with the displacement of the (y) screw, studying the behavior for the flexion movement (see Fig. 11(a)).
Analyzing the biomechanical results in comparison to the data of the flexibility sensors collected, we observed that there is no linearity (see Fig. 11(b)).

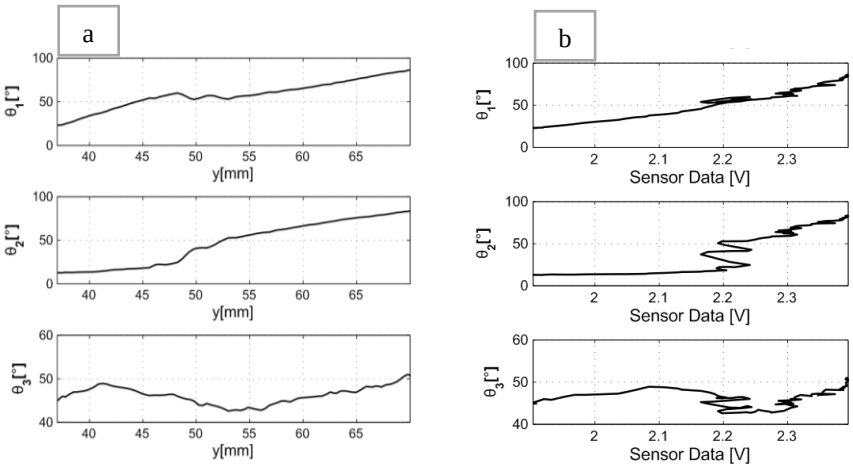

Figure 11. (a) Relation of the angles of joints between the finger phalanges with the worm screw dislocation for flexion movement. (b) Comparison between flexibility sensor data and biomechanical analysis data for flexion movement

Due to the complexities and nonlinearities obtained in the results, for our PID control system, we use the tuning process with the help of the "trial and error" method, due to the advantage of not having to know the system model that is sometimes very difficult to be determined. The PID control which is to the precise control of a variable in a system, allows us to operate stably at the desired set point, even occurring variations or disturbances that affect its stability.

The idea of position control is to ensure the position of each finger to obtain the desired posture of the robotic hand, the measured and conditioned (p_m) signals of the flexibility sensors and the potentiometers coupled to the motors are used to be compared with the reference value (p_d) for the control algorithm.

The possibility of estimating muscle strength from the EMG signal is attractive because it allows the assessment of the contributions of the individual muscles to the total force exerted by a muscle group. This is the main reason why EMG signals are and probably will always be the method of choice for estimating the force, approaching that the relationship between force and amplitude sEMG has been found to be linear (R.Merletti, P. Parker, 2004). We thus estimate the desired force (f_d) from the total energy of the E_W^T wavelet coefficients (see Eq. (8)) and consider (f_m) the measured force of the FSR sensor readings that were located in the palm of the hand.

The PID control algorithm was implemented in the FPGA of the compactRio 9012 which operates at the frequency of 10 kHz. The structure shown (see Fig. 12) is used for force control and position independent by using the control output to power the PWM system of the engine, which controls the movement of the fingers at a frequency of 1 kHz.

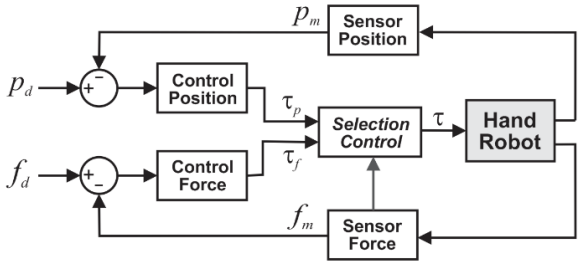

Figure 12. General diagram of the position and force control system.

It was proposed to control force with the help of the following rules:

- Establish the magnitude of the grip force of the robotic hand to tighten an object in a desired position.
- The robotic hand starts by operating in position control, moving in the free space until it reaches the desired position to begin the grip of the object. For now, the power control is off.
- The hand comes into contact with the object, and the force sensor starts to experience a small magnitude of the signal, thus initiating the force control operation and deactivating the position control.

6. EXPERIMENTS AND RESULT

It was integrated all the methods used and parts developed in this work, and with the help of a graphical environment developed in LabView, the methods were evaluated and adjusted, and also the systems of control of position and force of the robotic hand were tuned.

In the Figure 13, We can observe the different types of patterns that our system recognizes and experiences. For the "Spherical grasp" pattern our robotic system can control the force interacting with the object.

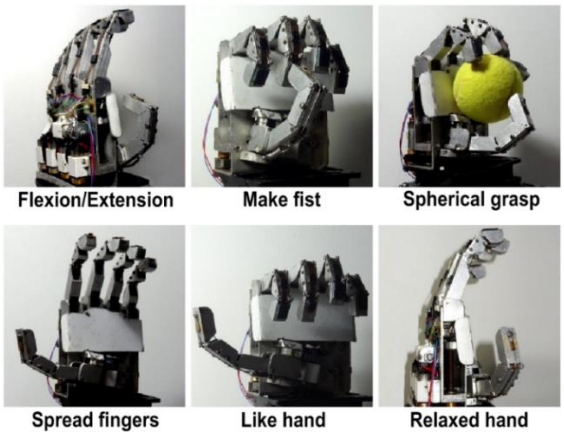

Figure 13. Analyzed positions of the robotic hand.

For force control use the desired value (f_d) estimated from the total energy of the coefficients wavelets E_W^T (see Eq. (8)), where we use the range of f_d to estimate *Force.k*.

In the Figure 14, we can observe the different control responses according to the different reference values of the desired force.

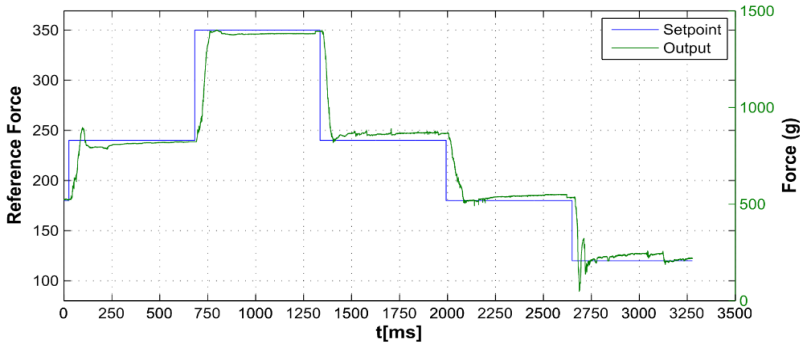

Figure 14. Force control response for different reference values.

By integrating all the parts and methods that conform the operation of the robotic hand we obtain a new table of results in the recognition for the three sets of patterns studied (see Tab. 5). The results improved in relation to the Tab. 4 because we added the sample validation method that we used to discriminate whether the collected signals are part of a standard under study or not.

Table 5. Final result of the neural network classification and sample analysis.

Pattern name	% Recognition		
	6 Patterns	5 Patterns	4 Patterns
Extension	88.5	89.5	94
Flexion	98	100	100
Like hand	97.5	95	94.5
Spherical	87	91.5	96.5
Make fist	94.5	95.5	-----
Spread	77.5	-----	-----
	90.50%	94.30%	96.25%

To estimate the processing time at each stage, a database was used for the recognition of five patterns. (Tab. 6).

Table 6. Time of robotic hand processes.

Processes	Time
Checking Data	54 µS
TWP	40 mS
MLP	11 µS
Total	40.07 ms

7. CONCLUSIONS

In this work, all the proposed objectives were fulfilled. Acquisition methods, methods of interpretation and processing of superficial electromyographic signals were developed. Also, the construction of a flexible robotic hand was developed, able to adapt to the morphology of the objects, developing strategies of position control and force to perform basic tasks.

The control algorithms of flexion and extension movement of the fingers and the power control algorithms of the robotic hand are controlled by sEMG signal and were implemented in the FPGA of CompactRIO 9012. The robotic hand was able to execute the desired commands of the individuals.

The proportional force control was able to provide adequate gripping force to the object through the measurement on the sensor located in the palm of the hand. The control is totally independent to the force control as to control the position of the fingers. The tuning of the controls was performed manually in the search for a better performance for the different patterns of the robotic hand positions.

A program was developed with the help of LabView software to perform communication between the robot actuators and the computer, to adjust the control parameters, to adjust some other parameters of the pre-processing step, and to visualize the degree of pattern recognition.

The NI CompactRio 9012 programmable controller complied with high performance, the data acquisition function for the collection of the electromyographic signals, and in the measurement of the sensors for the use of the control method. It has also satisfactorily fulfilled the real-time processing function, achieving the implementation of high-speed control methods in the programmable FPGA.

The total mass of the robotic hand structure, including the mass of the sensors, actuators and the transmission elements, results to be approximately 400 g. In addition, the size is approximately the size of the human hand, 6 DC motors as actuators, 8 sensors (6 position + 2 force) and 16 degrees of freedom were used. By which, the goal was to reduce mass and size without reducing the number of degrees of freedoms.

8. REFERENCES

Alan V. Oppenheim, 1997, “Signals and Sytems”, Second Edition. Published by Prentice-Hall.

Albert Malvino, 1998. Electronic Principles. Sixth Edition. McGraw-Hill, Febrary 1998.

Douglas G. Smith, 2006. “Amputee Coalition of America”. Publication in Motion, Vol. 16 - Issue 6.

Fahri V., Ayhan O., 2009. "Power parameters calculations based on wavelet packet transform". Journal: Electrical Power and Energy Systems 31 (2009), pp. 596–603.

G.L. Taylor, R.J.Schwart, 1955. “The Anatomy and Mechanics of the Human Hand, Artificial Limbs”, Vol.2, pp.22–35.

Ming Z., Kaicheng Li, Yisheng Hu., 2010. “Classification of Power Quality Disturbances Using Wavelet Packet Energy Entropy and LS-SVM”. Published Online August 2010. Energy and Power Engineering, 2010, pp. 154–160.

Peter Konrad, 2005. The ABC of EMG, A Practical Introduction to Kinesiological Electromyography. Noraxon, USA.

R.Merletti, P. Parker, 2004. "Electromyography, Physiology, Engineering and Noninvasive Applications". IEEE Press Engineering in Medicine and Biology Society, Sponsor.

Talles M. G., 2008. Uma Arquitetura de Redes de sensores do Corpo Humano. Tese de doutorado em engenharia elétrica. Universidade de Brasília - Faculdade de Tecnologia, PPGENE. TD-021/08.

Texas Instrument, 2000. Incorporated INA114 Precision Instrumentation Amplifier Datasheet.

Zecca M., Micera S., Carrozza M., 2002. "Control of Multifunctional Prosthetic Hands by Processing the Electromyographic Signal". ARTS Lab, Scuola Superiore Santanna, Pontedera, Italy.

9. RESPONSIBILITY NOTICE

The authors are the only responsible for the printed material included in this paper.